# High pressure X-ray diffraction study of $CaMnO_3$ perovskite*

LIU Ying-Xin(刘迎新)[1,2] QIN Shan(秦善)[2;1)] JIANG Jian-Zhong(蒋建中)[3]
Kikegawa Takumi[4] SHI Guang-Hai(施光海)[1]

[1] State Key Laboratory of Geological Processes and Mineral Resources, China University of Geosciences, Beijing 100083, China
[2] Department of Geology and Key Laboratory of Orogenic Belts and Crustal Evolution of MOE, Peking University, Beijing 100871, China
[3] International Center for New-Structured Materials (ICNSM), Zhejiang University and Laboratory of New-Structured Materials, Department of Materials Science and Engineering, Zhejiang University, Hangzhou 310027, China
[4] Institute of Materials Structure Science, High Energy Accelerator Research Organization, Tsukuba 3050801, Japan

**Abstract** Using a diamond anvil cell device and synchrotron radiation, the in-situ high-pressure structure of $CaMnO_3$ has been investigated. In the pressure up to 36.5 GPa, no pressure-induced phase transition is observed. The pressure dependence on the lattice parameters of $CaMnO_3$ is reported, and the relationship of the axial compression coefficients is $\beta_a > \beta_c > \beta_b$. The isothermal bulk modulus $K_{298}$=224 (25) GPa is also obtained by fitting the pressure-volume data using the Murnaghan equation of state.

**Key words** $CaMnO_3$, high-pressure, structure, phase transition, X-ray diffraction

**PACS** 91.60.Gf, 91.60.Fe, 91.60.Hg

## 1 Introduction

Many $ABO_3$ compounds with perovskite structure exhibit orthorhombic *Pnma* symmetry under ambient conditions, and are of particular interest to earth scientists due to perovskite-type (Mg, Fe)$SiO_3$, which is believed to be the most abundant mineral in the Earth's lower-mantle [1]. In this group of perovskites, calcium manganate is an excellent crystal chemical analogue for $MgSiO_3$ since both compounds are of $A^{2+}B^{4+}O_3$ type perovskite and $CaMnO_3$ is more persistent than $MgSiO_3$ when recovered under ambient conditions. Since the first X-ray diffraction was performed by Poeppelmeier [2], various experiments of $CaMnO_3$ have been carried out, such as electrical conductivity [3, 4], thermal conductivity [5, 6], magnetic properties [6–10], and structural characteristics under different conditions [11–14]. Up to now, no high-pressure experiments of $CaMnO_3$ have been found in the literature. $Mn^{4+}$ has an ionic radius of 0.53 Å, i.e., the same as that of $Ge^{4+}$ of 0.53 Å [15]. Therefore, it is reasonable to reference the high-pressure behavior of its analogue $CaGeO_3$ perovskite, which has the similar *Pnma* structure, in order to better understand the structure stability of $CaMnO_3$. The earliest high-pressure study suggested that the $CaGeO_3$ structure became less distorted as pressure increased, with a possible phase transition to a tetragonal structure at about 12.5 GPa, using extended X-ray absorption fine structure (EXAFS) [16]. A subsequent far-infrared study found no evidence of such a phase transition up to 24.4 GPa [17]. Ross and Angel studied the compressibility of $CaGeO_3$ single crystal in a Diamond Anvil Cell (DAC) at pressures up to 8.6 GPa, and gave the bulk modulus and its pressure derivative from the high-pressure data [18]. The latest high-pressure experiments of $CaGeO_3$ were carried out by Liu and Li, using ultrasonic interferometry in conjunction with synchrotron X-ray radiation [19]. They observed no discontinuities or elasticity softening for either the bulk or shear moduli up to the peak pressure of 10 GPa.

In this paper, we present the results of measurements of the compressional behavior and the unit cell

Received 17 September 2009, Revised 15 December 2009
* Supported by National Natural Science Foundation of China (40972029)
1) Corresponding author, E-mail: sqin@pku.edu.cn

parameters of $CaMnO_3$ perovskite as a function of pressure up to 36.5 GPa. The isothermal bulk modulus and its pressure derivatives are derived from the measured pressure-volume ($P-V$) data.

## 2 Experiments

The $CaMnO_3$ sample used in this study was synthesized with standard solid state methods. The reagents $CaCO_3$ and $MnO_2$ (Chempur, 99.9%) were dried for 5 hours at 500 ℃. Mixtures of stoichiometric amounts were heated form 500 to 1000 ℃ at a rate of 30 ℃ per hour, and then down to room temperature slowly in furnace. With periodic regrinding in an agate mortar, the samples were fired from 1000 to 1400 ℃ in air and kept at 1400 ℃ for at least 23 hours, then cooled rapidly in air to room temperature. The samples were then analyzed with a JEOL JXA-8100 electron microprobe (EMP), which was operating at an accelerating voltage of 15 kV and using a beam current of 10 nA with the diameter of 1 μm. A range of standard minerals from SPI was used for standardization and all data were reduced using the PHZ correction routine. The microprobe analysis showed that the real chemical composition was close to the nominal's (Table 1).

Table 1. Chemical composition of $CaMnO_3$. $\overline{x}$: average values over three EMP data.

| | $MnO_2$ | SrO | CaO | Mn (wt.%) | Sr (wt.%) | Ca (wt.%) | O (wt.%) | Mn/mol | Sr/mol | Ca/mol | O/mol |
|---|---|---|---|---|---|---|---|---|---|---|---|
| 1 | 60.780 | 0.049 | 39.180 | 38.41 | 4.14 | 28.00 | 33.56 | 1.000 | 0.001 | 0.999 | 3 |
| 2 | 60.040 | 0.024 | 39.070 | 37.94 | 2.03 | 27.92 | 33.25 | 0.997 | 0.000 | 1.006 | 3 |
| 3 | 61.140 | 0.028 | 39.100 | 38.64 | 2.37 | 27.94 | 33.66 | 1.003 | 0.000 | 0.994 | 3 |
| $\overline{x}$ | 60.65 | 0.034 | 39.117 | 38.33 | 2.85 | 27.96 | 33.49 | 1.000 | 0.000 | 1.000 | 3 |

The high-pressure angular dispersive X-ray diffraction (ADXD) measurement was performed at Beam Line 18C, KEK in Japan, with a 400 μm culet Mao-Bell DAC and an imaging plate detector. The X-ray beam was focused to a dimension of 60 μm×60 μm. Monochromatic synchrotron radiation at $\lambda$=0.6198 Å was used for data collection with $2\theta$ ranging between 5° and 25°. Eighteen runs up to 36.5 GPa were carried out. The typical exposure time of about 10 min was employed for a diffraction pattern at high pressures.

16:4:1 methanol-ethanol-water mixture was used as pressure medium in DAC. The $CaMnO_3$ sample was ground to powder in an agate mortar, and then loaded together with a ruby chip into a 120 μm hole drilled on a T301 stainless steel gasket, which was pressurized to 50 μm thick. The pressure was measured by the shift of the R1 photoluminescence line of ruby [20].

## 3 Results and discussion

In order to yield the intensity versus $2\theta$ plots, program WINPIP was used to process the two-dimensional ring patterns. Five selected patterns at different pressures are illustrated in Fig. 1. All these diffraction lines have been normalized and eliminated backgrounds. At normal atmospheric pressure, 17 diffraction peaks could be observed and indexed. No splitting or merging peaks are observed at elevated pressure and all these peaks are similar up to 36.5 GPa, which indicates that the structure of $CaMnO_3$ is *Pnma* (Fig. 1 and Fig. 2). Therefore, the qualitative phase analysis was performed by fitting the X-ray diffraction profile with the Rietveld method using the GSAS software [21]. The refined parameters were background coefficients, histogram scale factors, lattice parameters, linewidths, and atomic positions. *Pnma* structure calculated by Poeppelmeier was used as the initial structure model [2]. The fitting result was listed in Table 2, such as cell parameters and $R$ factors.

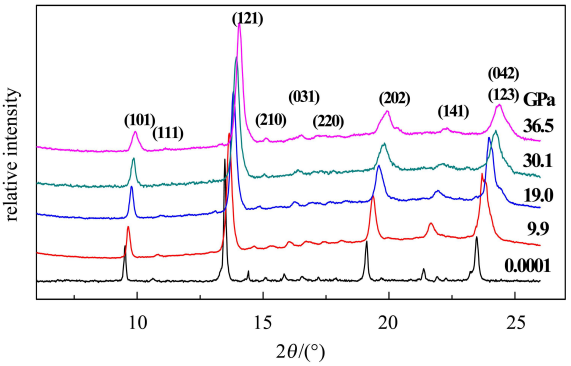


Fig. 1. The selected ADXD patterns of $CaMnO_3$ at different pressures. The numbers in parenthesis above the pattern are the corresponding Miller indices of $CaMnO_3$.

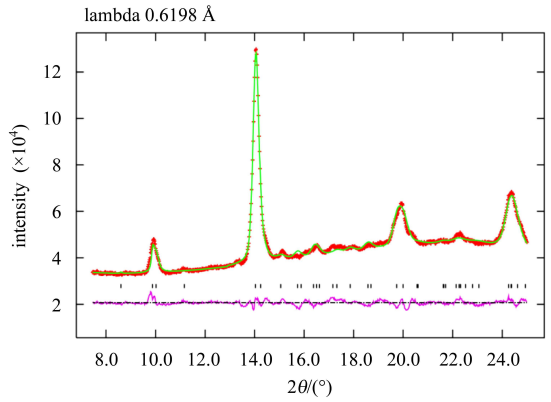


Fig. 2. The observed (shown as crosses), calculated (solid lines) and difference (solid lines) ADXD pattern of $CaMnO_3$ at 36.5 GPa. Tick marks indicate the calculated positions of *Pnma* peaks.

As shown in Table 2, the relationship between $a$ and $c$ axis changes from $a > c$ to $a < c$ when the pressure is above 10 GPa. A similar phenomenon has been observed by Kennedy [22] and Mountstevens [23], who believed it implies a $Pnma \rightarrow Imma$ phase transition. Therefore, we used the *Imma* structural model to refine the high-pressure structure. However, the refinement was not converged and high $R$ values were obtained, which means *Imma* is not the appropriate high-pressure structure. Due to the non-hydrostatic environments of 4:1 methanol-ethanol mixture above 10 GPa at room tempreature [24], the abnormal change of $a$ and $c$ is probably caused by the solidification of the pressure medium.

Table 2. Cell parameters of $CaMnO_3$ as a function of pressure. The numbers in the parentheses are the estimated standard deviation in units of the last digit(s).

| $P$/GPa | $a$/Å | $b$/Å | $c$/Å | $V$/Å$^3$ | space group | $R_p$ | $_wR_p$ |
|---|---|---|---|---|---|---|---|
| 0.0001 | 5.2855(14) | 7.4504(18) | 5.2826(15) | 208.0(1) | *Pnma* | 1.46 | 2.26 |
| 0.9 | 5.2852(45) | 7.4366(16) | 5.2820(47) | 207.6(1) | *Pnma* | 1.53 | 2.32 |
| 2.9 | 5.2599(26) | 7.4004(21) | 5.2782(34) | 205.4(1) | *Pnma* | 1.80 | 2.57 |
| 6.5 | 5.2483(44) | 7.3855(19) | 5.2479(55) | 202.6(1) | *Pnma* | 2.19 | 3.12 |
| 8.0 | 5.2450(38) | 7.3746(19) | 5.2361(40) | 202.5(2) | *Pnma* | 2.02 | 2.85 |
| 9.9 | 5.2382(25) | 7.3524(35) | 5.1983(29) | 200.2(2) | *Pnma* | 1.90 | 2.91 |
| 13.2 | 5.1841(30) | 7.3503(24) | 5.1989(36) | 196.8(2) | *Pnma* | 1.91 | 2.50 |
| 15.3 | 5.1425(20) | 7.3456(23) | 5.1920(23) | 196.7(1) | *Pnma* | 1.86 | 2.66 |
| 19.0 | 5.1232(22) | 7.3372(25) | 5.1690(30) | 194.3(1) | *Pnma* | 2.00 | 2.95 |
| 21.5 | 5.1169(50) | 7.2965(40) | 5.1650(28) | 193.7(2) | *Pnma* | 2.09 | 2.90 |
| 26.3 | 5.0903(25) | 7.2848(31) | 5.1606(28) | 191.4(2) | *Pnma* | 2.15 | 2.98 |
| 27.6 | 5.0790(19) | 7.2817(25) | 5.1426(20) | 190.2(1) | *Pnma* | 1.50 | 2.27 |
| 30.1 | 5.0688(24) | 7.2627(31) | 5.1279(22) | 187.3(2) | *Pnma* | 2.11 | 2.80 |
| 33.0 | 5.0586(37) | 7.2052(37) | 5.1207(28) | 186.6(2) | *Pnma* | 1.85 | 2.58 |
| 36.5 | 5.0330(32) | 7.2048(28) | 5.1070(23) | 186.7(2) | *Pnma* | 1.51 | 2.03 |

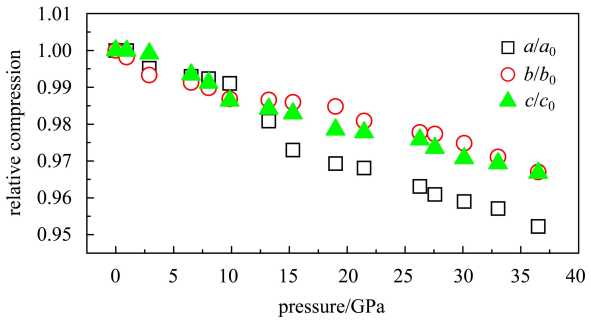


Fig. 3. Relative compression of $CaMnO_3$, shows the variation of relative axial ratios as a function of pressure.

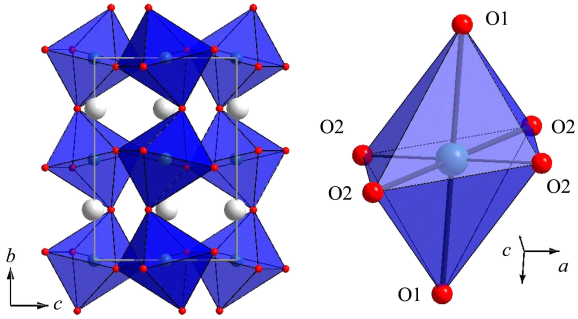


Fig. 4. The crystal structure of $CaMnO_3$ (left, large circles stand for Ca atom and polyhedra stand for $MnO_6$ octahedra) and $MnO_6$ octahedron (right, large circles stand for Mn atom and small ones are O atom) at 36.5 GPa.

The relative compression of unit cell parameters is plotted in Fig. 3. As shown in the figure, the compression behavior looks similar along the three crystallographic axes. It can be distinguished that the less compressible axes are the $b$ and $c$, while the $a$ axis is more compressible. The compression ratios are $\beta_a$=1.31×10$^{-3}$ GPa$^{-1}$, $\beta_b$=0.90×10$^{-3}$ GPa$^{-1}$, $\beta_c$=0.93×10$^{-3}$ GPa$^{-1}$ respectively, with $\beta_a$:$\beta_b$:$\beta_c$=1:0.69:0.71. According to the GSAS refinement, the average bond distance of Mn-O1 is 1.8875 Å, 1.6501 Å and 2.2087 Å of Mn-O2 at normal atmospheric pressure. When the pressure is up to 36.5 GPa, these bond distances change to 1.9182 Å, 1.4257 Å and 2.2542 Å respectively, which means that the distortion of $MnO_6$ octahedra increased. It can be seen from Fig. 4 that the shortest Mn-O2 bond in $MnO_6$ octahedron is almost parallel to $a$ axis. This may be the reason for the most compression along the $a$ axis.

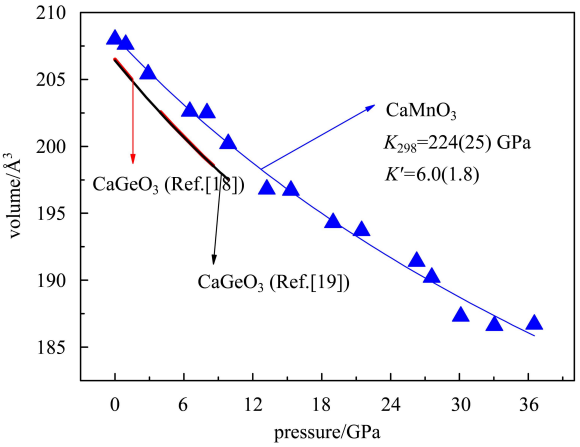


Fig. 5. Pressure dependence of unit cell volume. The $CaMnO_3$ curve fitted to the Murnaghan equation of state is shown with a thin solid line. The heavy lines represent $CaGeO_3$ data from Refs. [18, 19].

The Murnaghan EOS

$$P=\frac{K_0}{K_0'}\left[\left(\frac{V_0}{V}\right)^{K_0'}-1\right]$$

was used to fit the $P$–$V$ data. The calculating results are isothermal bulk modulus $K_{298}$=224 (25) GPa with $K'$=6.0 (1.8), which shows that $CaMnO_3$ has a similar compressive behavior to $CaGeO_3$ [18, 19] (Fig. 5).

## 4 Conclusions

The in-situ high-pressure structures of $CaMnO_3$ (Pnma) have been investigated using ADXD and DAC techniques under pressures up to 36.5 GPa. The experimental results confirm $CaMnO_3$ has no phase transition in this pressure range. By a linear fitting, the axial compression coefficients of $CaMnO_3$ are obtained as $\beta_a$=1.31×10$^{-3}$ GPa$^{-1}$, $\beta_b$=0.90×10$^{-3}$ GPa$^{-1}$, $\beta_c$=0.93×10$^{-3}$ GPa$^{-1}$ respectively. The reason why $a$ axis is the most compressible is explained from the high-pressure structure behavior of $CaMnO_3$. The pressure dependence of cell volume is fitted to the Murnaghan EOS, yielding a room-temperature isothermal bulk modulus $K_{298}$=224 (25) GPa.

## References


1 Kinttle E, Jeanloz R. Science, 1987, **235**: 668
2 Poeppelmeier K R, Leonowicz M E, Scanlon J C et al. Journal of Solid State Chemistry, 1982, **45**: 71
3 Taguchi H, Sonoda M, Nagao M. Journal of Solid State Chemistry, 1998, **137**: 82
4 Moure C, Villegas M, Fernandez J F et al. Journal of Materials Science, 1999, **34**: 2565
5 Chmaissem O, Dabrowski B, Kolesnik S et al. Physical Review B, 2001, **64**: 134412/1
6 Fujishiro H, Fujine Y, Mita Y et al. Journal of Magnetism and Magnetic Materials, 2004, **272-276**: 1796
7 Schiffer P, Ramirez A P, Bao W et al. Physical Review Letters, 1995, **75**: 3336
8 Neumeier J J, Cohn J L. Physics Review B, 2000, **61**: 14319
9 Töpfer J, Pippardt U, Voigt I et al. Solid State Sciences, 2004, **6**: 647
10 Jin S, Tiefel T H, McCormack M et al. Science, 1994, **264**: 413
11 Liarokapis E, Leventouri Th, Lampakis D et al. Physical Review B, 1999, **60**: 12758
12 Abrashev M V, Bäckström J, Börjesson L et al. Physical Review B, 2002, **65**: 184301/1
13 Taguchi H, Nagao M, Santo T et al. Journal of Solid State Chemisray, 1989, **78**: 312
14 Zhou Q D, Kennedy B J. Journal of Physics and Chemistry of Solids, 2006, **67**: 1595
15 Shannon R D. Acta Crystallographica A, 1976, **32**: 751
16 Andrault D, Poirier J P. Physics and Chemistry of Minerals, 1991, **18:** 91
17 Lu R, Hofmeister M. Physics and Chemistry of Minerals, 1994, **21**: 78
18 Ross N L, Angel R J. American Mineralogist, 1999, **84**: 277
19 Liu W, Li B S. Physical Review B, 2007, **75**: 024107/1
20 Barnett J D, Block S, Piermarini G J. Review of Scientific Instrument, 1973, **44**: 1
21 Larson A C, Von Dreele R B. GSAS: General Structural Analysis System, LANSCE. Los Alamos National Laboratory, Los Alamos, NM, The Regents of the University of California,1994
22 Kennedy B J, Howard C J, Thorogood G J et al. Journal of Solid State Chemistry, 2001, **161**: 106
23 Mountstevens E H, Attfield J P, Redfern S A T et al. Journal of Physics: Condensed Matter, 2003, **15**: 8315
24 Piermarni G J, Block S, Barnerr J D. Journal of Applied Physics, 1973, **44**: 5377